Heliyon 10 (2024) e31383

Contents lists available at ScienceDirect

Heliyon

journal homepage: www.cell.com/heliyon

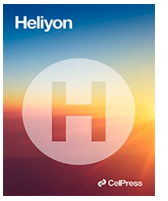

Research article

Evaluafion of the efficacy of wall shear stress in carotid artery stenting

Tao Xiaoyong [a,1], Chen Yuping [a,1], Huang Wei [a], Chen Juan [a], Qiu Feng [a,*], Li Zhuo [b,**]

[a] Senior Department of Neurology, The First Medical Center of PLA General Hospital, Beijing, China
[b] Department of Ultrasonography, The Eighth Medical Center of PLA General Hospital, Beijing, China

ARTICLE INFO

Keywords:
Carotid artery stenosis
Stenting
Flow vector imaging
Wall shear stress
Ischemic stroke

[ABSTRACT]

Objective: To characterize the value of carotid wall shear stress (WSS) following carotid artery stenting (CAS) in patients with carotid stenosis.
Methods: Twenty-eight patients with carotid stenosis treated with CAS between March 2021 to May 2022 in the eighth medical center of the PLA General Hospital were selected for our study. Carotid ultrasound was performed before the operation, one week post-operation, and six months post-operation. Carotid artery WSS was detected by blood flow vector imaging, and the changes in WSS before and after the operation were collected. Genetic testing of drugs was detected for patients with restenosis.
Results: Pre-operative WSS of the proximal, narrowest region, and distal carotid arteries in patients with ischemic carotid artery stenosis was 7.88 ± 3.18Pa, 14.36 ± 6.66Pa, and 1.55 ± 1.15Pa, respectively. Comparatively, pre-operative WSS of the proximal, narrowest region and distal carotid arteries in patients without ischemic symptoms was 5.02 ± 1.99Pa, 9.68 ± 4.23Pa, and 1.10 ± 0.68Pa, respectively, with a significant difference between the two groups ($p < 0.001$). Overall WSS of the proximal, narrowest region, and distal carotid arteries in patients before CAS was 6.68 ± 3.0Pa, 12.47 ± 5.98Pa, and 1.39 ± 0. 96Pa. WSS of the proximal, narrowest region, and distal carotid was 4.15 ± 1.42Pa, 6.71 ± 2.64Pa, and1.86 ± 1.13Pa one week after CAS, compared to 4.44 ± 1.91Pa, 7.90 ± 4.38Pa, and 2. 36 ± 1.09Pa six months after CAS. WSS of the proximal and narrowest region of the carotid artery was reduced after carotid stenting, and the difference was statistically significant ($p < 0.001$). There was no statistically significant difference in WSS between one week and six months after stenting ($P > 0.05$).
Conclusion: We employed early carotid WSS as a means of evaluating the efficacy of carotid artery stenting. Changes in carotid WSS are closely associated with carotid artery stenosis, providing valuable hemodynamic information for CAS treatment. This technique holds great application value in pre-operative evaluation and long-term follow-up.

* Corresponding author.
** Corresponding author.
E-mail address: qiufengnet@hotmail.com (Q. Feng).
[1] Contributed equally.

https://doi.org/10.1016/j.heliyon.2024.e31383
Received 21 September 2023; Received in revised form 14 May 2024; Accepted 15 May 2024
Available online 18 May 2024

1. Introduction

Carotid artery stenosis and ischemic stroke are intimately linked, with about 20 % of strokes caused by extracranial carotid artery stenosis [1,2]. Over time, symptomatic patients with 50%–70 % stenosis exhibit a history of transient ischemic attack (TIA) or cerebral infarction, and for asymptomatic patients with 70%–99 % stenosis, stenting has become a mainstay treatment [3]. The most common cause of carotid artery stenosis is arteriosclerosis, and the evolution of arteriosclerotic plaque is closely linked to local hemodynamics factors. WSS is the frictional force exerted in parallel to the endothelial surface of the vessel wall by blood viscosity. It is considered a major parameter to assess the risk of atherosclerosis. Traditional color Doppler ultrasound imaging provides accurate data on the velocity component of blood flow only under the laminar flow condition.However, it is challenging to obtain the correct blood flow velocity component for WSS calculations in complex blood flow scenarios. The v-flow technique, on the other hand, can provide directional information about blood flow velocity and aid in obtaining precise blood flow velocity components for more accurate WSS evaluation [4].

Studies have shown that low carotid WSS can lead to increased blood retention at the carotid artery, resulting in the enhanced deposition of lipoproteins. At the same time, the production of vascular endothelium damaging factors can increase while that of the protective factors can decrease, thereby promoting the development of arteriosclerosis. Increased WSS can inhibit platelet-derived growth factor (PDGF) secretion, reduce vascular smooth muscle protein synthesis, and inhibit vascular endothelial cell proliferation, ultimately leading to thinning and rupture of the arteriosclerotic plaque fibrous cap [5–11].

WSS in the carotid artery is typically measured using MRI or enhanced CT with 3D reconstruction software. Flow vector imaging enables visualization of blood flow and hemodynamics, allowing for the detection of WSS, eddy currents, and countercurrents. This technique is extensively employed in the diagnosis of cardiovascular diseases and the evaluation of treatments [12–15].WSS was utilized for quantitative analysis before and after treatment in type B aortic dissection [16]. It was also applied in evaluating the risk of rupture for thoracic aortic aneurysms, as well as aneurysms at the carotid artery bifurcation region [17].Vector flow imaging (VFI) is angle-independent, providing intuitive images of vortex formation and enabling assessment of blood flow patterns at the carotid bifurcation [4,18]. Moerman et al. conducted MRI imaging of carotid bifurcations in CEA patients, comparing WSS metrics and plaque vulnerability characteristics. Their findings revealed larger necrotic cores and macrophage activation in areas with high WSS and low oscillatory shear index areas [19].More recently, flow vector imaging to assess arteriosclerotic carotid artery stenosis hemodynamics has been increasingly studied [4].

At present, there are few studies characterizing changes in WSS after CAS. As such, the purpose of this study was to analyze changes in WSS in patients with carotid artery stenosis before and after CAS.To investigate the variation of WSS in different segments of stenosis and to understand the relationship between the magnitude of WSS and the degree of stenosis.

2. Patients and methods

2.1. Patients

A total of 28 patients with carotid artery stenosis were selected from the Department of Neurology of the Eighth Medical Center of PLA General Hospital, Beijing, China, between March 2021 and May 2022.

Inclusion criteria: Internal carotid artery stenosis confirmed to be 50 %–99 % by carotid ultrasound and cranial magnetic resonance angiography (MRA) or cranial computed tomographic angiography (CTA) or angiography due to arteriosclerotic changes. Among them, patients with 50%–70 % stenosis presented a history of TIA or cerebral infarction. Diagnostic criteria were based on the NASCET carotid endarterectomy trial [20]. Wall shear testing was performed preoperatively, after which patients' informed consent to participate in our study was obtained.

Exclusion criteria: (1) allergy to iodine contrast medium, (2) severe systemic organic diseases of the heart, liver, or lung (3) severe bleeding tendency and thrombocytopenia, (4) complete occlusion of the carotid artery, (5) prior carotid endarterectomy, (6) Non-atherosclerotic carotid artery stenosis, and (7) patients who could not undergo CAS due to other conditions.

2.2. Pre-operative preparation

Patients were given oral clopidogrel (75 mg/d) and aspirin (100 mg/d), as well as atorvastatin calcium tablets (20–40 mg/d) at least seven days before the operation. Patients fasted and were deprived of water 6 h before the operation. Blood routine examinations, blood glucose level, liver and kidney function, myocardial enzymes, electrolytes, coagulation status, ECG, and cardiac function evaluation were collected and performed before the operation.

2.3. WSS examination

Using a Resona9 Color Doppler Ultrasound Diagnostic Apparatus (Shenzhen Mindray Biomedical Electronics Co. Ltd., Shenzhen, China), patients were positioned in the supine position with their necks fully exposed. The largest longitudinal section of the middle segment of the common carotid artery was identified. The lumen of the common carotid artery was centered at the middle of the sampling frame in the horizontal Flow imaging mode. While keeping the probe still for 1.5 s, the "Update" button was then pressed to store V-Flow dynamic images. Flow dynamic images were collected at the proximal, narrowest, and most distal longitudinal sections of the carotid artery. The images were stored and analyzed, and the average WSS of the proximal, narrowest, and distal segments of

interest were measured. More specifically, each of the proximal, narrowest, and distal sections of the carotid artery was divided artificially into six sections, and the average of six wall stress measurements was calculated to give the mean WSS. Wall shear tests were performed preoperatively, one week post-operatively, and six months post-operatively.

In the V-flow mode, high velocities were represented by red vectors, medium velocities by yellow and orange vectors, and low velocities by green vectors. The length of the vector arrow represents the flow velocity. The WSS value is calculated by the following:

$$\overrightarrow{\tau}^{(t)} = \mu \sum_{i=1}^{i=N} \frac{\overrightarrow{w} . \overrightarrow{v_i}^{(t)}}{\Delta r_i}$$

Where τ is WSS, μ is blood viscosity; $\overrightarrow{w}$ denotes the direction of $\overrightarrow{\tau}$ and is a unit vector; $\overrightarrow{v_i}$ is the vector velocity; N is the number of velocities used for WSS estimation; Δ r_i is the distance from the *i*th velocity measurement to the WSS measurement location [21].

2.4. Carotid artery stenting

After local anesthesia, the femoral artery was punctured using Seldinger's technique, and an 8F arterial sheath was inserted. Utilizing a 0.035 inch misgurnus guide wire, the 8F guide catheter was positioned in the middle segment of the common carotid artery of the affected side, and the umbrella was sent through the stenosis along the guide wire to the distal part of C1 segment and released. After the balloon was removed, the self-expanding stent was inserted into the carotid artery. After the stent was released, the stent delivery system was removed.

2.5. Statistical analysis

Data were processed using SPSS 26.0 software. Continuous data were consistent with the homogeneity of variance of the normal distribution. Continuous data between two groups were compared using independent-sample t-tests, and within-group comparisons at different time points were compared using repeated-measures analysis of variance, presented as mean ± standard deviation. Two-sided t-tests were deemed significant with $p < 0.05$.

3. Results

3.1. Patients characteristics

A total of 28 patients were enrolled, including 24 males and 4 females. The average age was 67.11 ± 7.87 years, with a full range from 54 to 79 years old. Among the 28 participants, 2 had experienced transient ischemic attacks from the carotid system, 13 had experienced cerebral infarction, and 13 had asymptomatic carotid stenosis. 19 participants had hypertension, 15 had diabetes, 14 had coronary atherosclerotic heart disease, 8 had hyperlipidemia, and 7 had a history of cerebral infarction. All patients were examined using cervical vascular ultrasound and transcranial Doppler ultrasound, as well as head MRI, MRA, or CTA before the operation. All patients underwent cerebral angiography to confirm carotid artery stenosis, all of which were deemed moderate to severe stenosis.

Table 1
The baseline data of stenotic carotid artery patients.

	With ischemic symptoms	without ischemic symptoms	Total(P Value)
Age (year)			67.11 ± 7.87
Sex			0.4863
Female	1	3	4
Male	14	10	24
Side of the carotid artery			0.4120
Right	7	9	16
Left	8	4	12
Clinical symptoms			
Transient ischemic attack	2		2
Cerebral infarction	13		13
Asymptomatic		13	13
History			0.2362
Hypertension	12	7	19
Diabetes	6	9	15
Coronary heart disease	8	6	14
Hyperlipidemia	7	1	8
Cerebral infarction	5	2	7
DSA findings			0.7942
Moderate carotid stenosis	5	4	9
Severe carotid stenosis	10	9	19
Location			0.5883
Internal carotid artery	2	3	5
Carotid bifurcation	15	8	23

Stenosis was located at the end of the common carotid artery and the initial segment of the internal carotid artery in 23 cases, a simple initial segment of the internal carotid artery in 5 cases, and bilateral internal carotid artery stenosis in 3 cases (Table 1).

3.2. Wall shear stress examination

The degree of carotid stenosis was 50 %–69 % in 9 of 28 patients. WSS in the proximal, narrowest, and distal regions of the stenosis was 4.78 ± 2.63Pa, 8.43 ± 4.19 Pa, and 1.39 ± 1.38 Pa, respectively. 19 patients had 70 %–99 % carotid stenosis, with proximal, narrowest, and distal WSS of 7.38 ± 2 88 Pa, 13.97 ± 6.05 Pa, and 1.32 ± 0.75 Pa. WSS at the proximal and narrowest regions of the stenosis was significantly increased based on the severity of the stenosis. WSS at the distal end of the stenosis decreased, with no statistically significant difference between the two groups (Table 2). In the 15 patients with cerebral infarction or transient ischemic attack, WSS of the proximal, narrowest, and distal regions of stenosis were 7.88 ± 3.18 Pa, 14. 36 ± 6. 66 Pa, and 1.55 ± 1.15 Pa, respectively. In the 13 patients without ischemic symptoms, the WSS in the proximal, narrowest, and distal parts of stenosis were 5.02 ± 1.99 Pa, 9.68 ± 4.23 Pa, and 1.10 ± 0.68 Pa, respectively. Compared to the patients without ischemic symptoms, the WSS in the proximal and narrowest parts of stenosis in patients with carotid stenosis accompanied by ischemic symptoms was significantly increased. WSS in the distal parts of stenosis was also increased, albeit without statistical significance (Table 3).

3.3. Comparison of carotid wall shear stress before and after stenting

Before the operation, the shear wall stress of the proximal, narrowest, and distal portions of stenosis in the 28 patients was 6.68 ± 3.35 Pa, 12.47 ± 5.98 Pa, and 1.39 ± 0. 96 Pa, respectively. Ultrasound examination showed that the degree of stenosis was less than 50 % within one week after stenting, and the shear stress of the proximal, narrowest, and distal sections was 4.15 ± 1.42 Pa, 6.71 ± 2.76 Pa, and 1.86 ± 1.13 Pa. Compared with pre-operative results, the WSS of the proximal and narrowest area of stenosis decreased one week after the operation, while the distal WSS increased, all with statistical significance. Six months after stenting, ultrasound showed that the degree of stenosis in 27 patients was less than 50 % and more than 50 % in 1 patient. Shear wall stress at the proximal, narrowest, and distal portions was 4.44 ± 1.91 Pa, 7.90 ± 4.38 Pa, and 2.44 ± 1.09 Pa, respectively. Compared to preoperatively, WSS at the proximal and narrowest regions of stenosis was decreased, while WSS at the distal region was increased at six months post-operation. All differences were statistically significant. There was no statistically significant difference in shear wall stress of the proximal, narrowest, and distal sections between six months and one week post-operatively (Table 4). Representative pre-operative and post-operative images of carotid WSS are shown in Figs. 1–3.

4. Discussion

WSS is a significant factor in the development of carotid atherosclerosis, and there is a strong correlation between carotid atherosclerosis and WSS. Patients with carotid artery stenosis are at higher risk of experiencing acute ischemic cerebrovascular events due to increased WSS. Evaluating WSS and the severity of stenosis together can help determine the risk level for patients with asymptomatic carotid artery stenosis [22]. Kamimura's findings suggest that reduced carotid WSS, as identified by vascular vector flow mapping, is associated with early-stage changes in imaging and cognition in small vessel disease [23]. Research conducted by Lan He demonstrates the promising potential of Vascular VFM technology in accurately assessing hemodynamic differences in the vascular flow field between patients with hypertension and normal controls. Variations in WSS levels could serve as an indicator for the risk of developing arteriosclerosis [24]. Nevertheless, there is limited research specifically focused on patients undergoing CAS.

Our findings that WSS is increased in the distal and lower in the proximal portions of carotid artery stenosis further suggests that decreased proximal WSS may aggravate intima-media thickening and promote plaque formation, and increased distal wall shear may increase the risk of plaque rupture. Compared with patients with carotid artery stenosis without ischemic symptoms, patients with ischemic symptoms had higher WSS proximal and at the narrowest portion of stenosis, indicating that the higher the WSS in the narrowest area, the greater the risk of plaque rupture and detachment. This is in line with the literature reporting that wall shear obtained by measuring peak systolic velocity at the narrowest portion of stenosis can be a better predictor of ischemic stroke than the degree of stricture [25,26].

The results also showed that the patients with 70 %–99 % stenosis had higher WSS in the proximal and narrowest regions compared to patients with 50 %–69 % stenosis, indicating a positive correlation between WSS and severity of stenosis, consistent with the literature [19]. After stenting, WSS decreased in the proximal and narrowest region, with a larger decrease in the narrowest region. There was no significant change in WSS of the proximal, narrowest, or distal regions six months post-operation compared with one week post-operation. In 1 of 28 cases, the WSS of the proximal and narrowest regions increased significantly. In this single case, the blood flow velocity increased, the vortex ratio increased, and the degree of stenosis was 70 %. The restenosis was indicated by

Table 2
Wall shear stress in patients with different degrees of stenosis.

Locations	50–69 %	70–99 %	t	P
Proximal of stenosis (Pa)	4.78 ± 2.63	7.38 ± 2.88	−2.292	0.030
Narrowest region of the carotid artery (Pa)	8.43 ± 4.19	13.97 ± 6.05	−2.471	0.020
Distal of stenosis (Pa)	1.39 ± 1.38	1.32 ± 0.75	−0.179	0.859

Table 3
Wall shear stress in patients with or without ischemic symptoms.

Locations	without	with	t	P
Proximal of stenosis (Pa)	5.02 ± 1.99	7.88 ± 3.18	−2.799	0.010
Narrowest region of the carotid artery (Pa)	9.68 ± 4.23	14.36 ± 6.66	−2.178	0.039
Distal of stenosis (Pa)	1.10 ± 0.68	1.55 ± 1.15	−1.251	0.222

Table 4
Comparison of wall shear stress before and after stenting.

Locations	Time			F	P
	pre-operative	1 week post-operatively	6 months post-operatively		
Proximal of stenosis (Pa)	6.68 ± 3.0	4.15 ± 1.42[a]	4.44 ± 1.91[a,b]	27.276	<0.001
Narrowest region of the carotid artery (Pa)	12.47 ± 5.98	6.71 ± 2.64[a]	7.90 ± 4.38[a,b]	25.725	<0.001
Distal of stenosis (Pa)	1.39 ± 0.96	1.86 ± 1.13[a]	2.36 ± 1.09[a,b]	19.995	<0.001

Note: for pairwise comparisons.
[a] Indicates $P < 0.05$ compared to shear stress pre-operative.
[b] Indicates $P > 0.05$ compared to shear stress 1 week post-operatively.

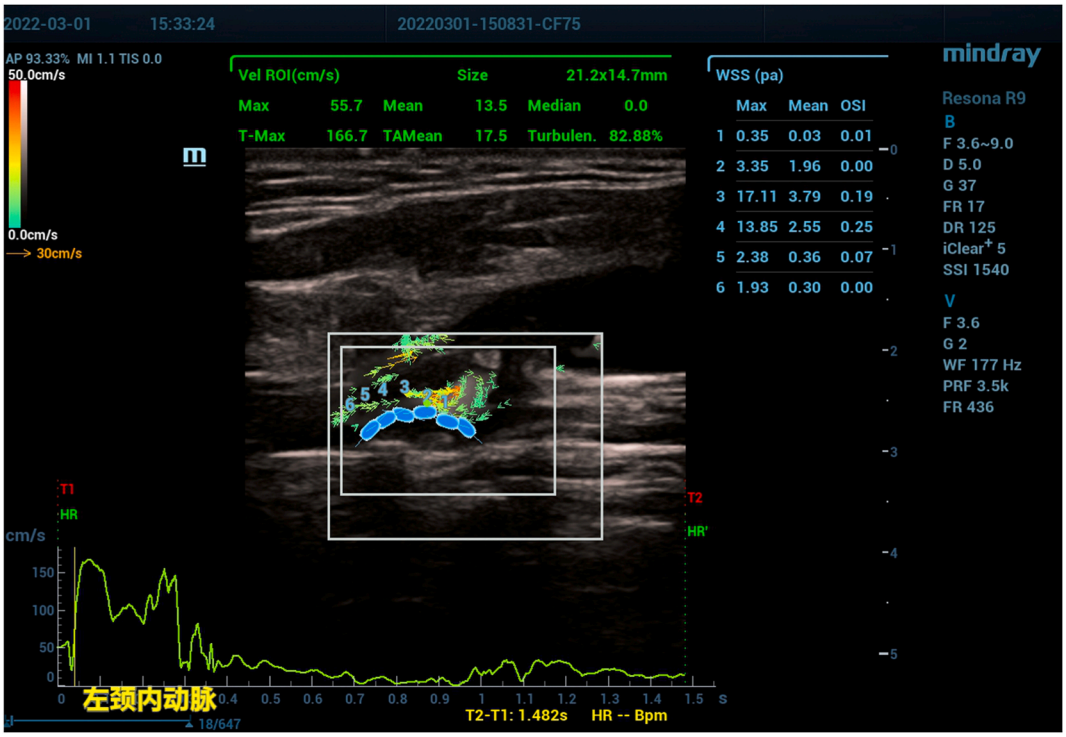

Fig. 1. Pre-operative v-flow imaging showed high-velocity flow (red vectors) at the narrowest region. WSS measurements exhibited a maximum WSS (WSSmax) value of 17.11Pa at the narrowest region and abnormally low WSSmax values were detected at the proximal (0.35Pa) and distal (1.93Pa) regions.

angiography. Notably, the case's gene analysis showed that the genotype for clopidogrel was CYP2C19 * 2/* 17, and the genotype for statins was SLCO1B1 * 1a/* 1b, apoe E3E4. In order for clopidogrel to exert its antiplatelet aggregation effects, it needs to be metabolized into active metabolites in the liver and bind to receptors on the platelet surface. Genetic variations, such as those in the CYP2C19 gene, can impact the antiplatelet efficacy of clopidogrel. The CYP2C19 gene displays high polymorphism, with the CYP2C19*2 variant being the predominant allelic variant linked to CYP2C19 enzyme deficiency and reduced enzyme activity. Carriers of such allelic variants experience slower clopidogrel metabolism and decreased antiplatelet aggregation effects [27]. Similarly, genes like SLCO1B1 and ApoE play a vital role in individual variations in the response to statin drugs. Polymorphisms in the SLCO1B1 gene influence the blood drug concentration of statins, while polymorphisms in the ApoE gene affect serum TC and TG levels, thereby impacting the lipid-lowering effects of statins. ApoE E4 exhibits the highest affinity with LDL-R, and carriers of ApoE E4 often have

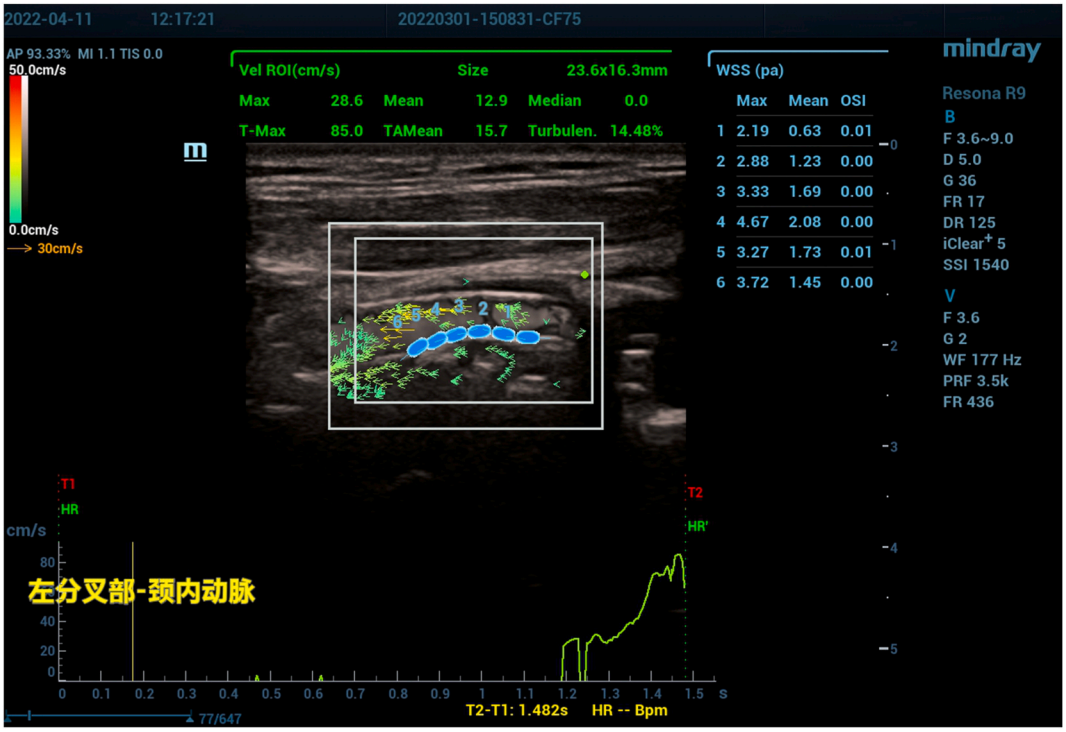

Fig. 2. One week after CAS, the v-flow imaging showed that the flow velocity returned to normal at the narrowest region. While WSS measurements revealed that the WSSmax could decrease significantly at the narrowest region and the WSSmax values at the proximal and distal regions were returned to normal.

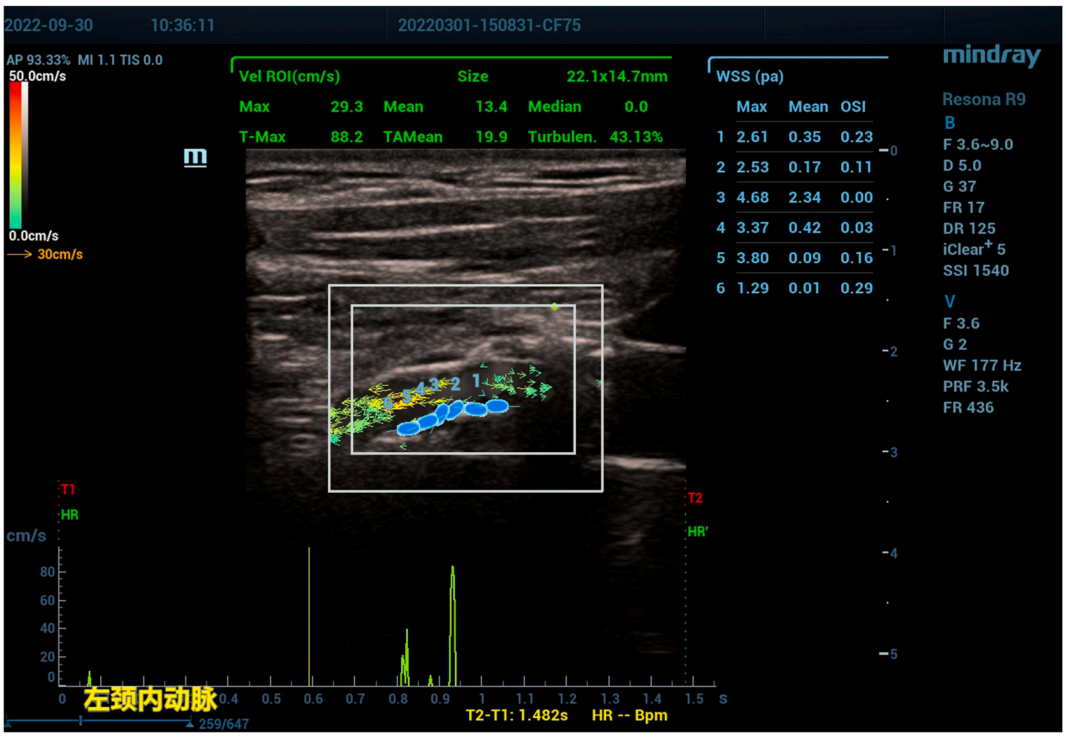

Fig. 3. Six months after CAS, there was no significant change in blood flow velocity at the narrowest region compared to that of one-week post-CAS. The WSSmax values at the narrowest proximal and distal regions were not significantly different, compared to those at one-week post-CAS.

higher lipid levels and may not respond well, or at all, to statin therapy [28,29].The patient is currently under follow-up after being transitioned from clopidogrel to ticagrelor and having ezetimibe added as a lipid-lowering drug along with atorvastatin calcium.

At present, the application of blood flow vector imaging to measure WSS of the carotid arteries is rare in the clinical setting. Notably, this is a self-contrast study. The number of cases included in this study is small and only from a single center, which limits the generalizability of our results. WSS affects the morphology, intimal proliferation, differentiation, metabolism, and communication of endothelial cells [30]. By controlling the near-wall transport processes involved in atherosclerosis, such as low-density lipoprotein, nitric oxide, adenosine triphosphate, oxygen, monocyte chemoattractant protein-1, etc. [31]. Our study did not examine the relationships between WSS, endothelial cells, and related biochemical mass transport models. Further studies are needed to understand the long-term value of WSS testing post-CAS because the technique has yet to be compared to repeat cerebral angiography, particularly in regard to in-stent restenosis.

In conclusion, ultrasonic measurement of WSS provides important hemodynamic information in patients with carotid artery stenosis before stent implantation to help determine severity and treatment options. The therapeutic effect can be evaluated after stenting, providing key long-term follow-up value.

Ethics approval and consent to participate

The study was conducted according to the guidelines of the Declaration of Helsinki and approved by The First Medical Center of PLA General Hospital Ethics Committee. All participants read a participant information sheet and provided informed consent prior to the interview. All methods were carried out in accordance with relevant guidelines and regulations.

Consent for publication

Not applicable.

Availability of data and materials

Original data to support the results of this study are not publicly available due to privacy reasons of patients, but are available from the corresponding author upon reasonable request.

CRediT authorship contribution statement

Tao Xiaoyong: Writing – original draft, Project administration, Methodology, Conceptualization. **Chen Yuping:** Project administration, Methodology, Investigation, Conceptualization. **Huang Wei:** Writing – original draft, Data curation. **Chen Juan:** Data curation. **Qiu Feng:** Writing – review & editing, Project administration, Methodology, Investigation, Conceptualization. **Li Zhuo:** Project administration, Methodology, Conceptualization.

Declaration of competing interest

The authors declare that they have no known competing financial interests or personal relationships that could have appeared to influence the work reported in this paper.

Acknowledgements

None.

References

[1] A.N. Alagoz, B.A. Acar, T. Acar, A. Karacan, B.E. Demiryurek, Relationship between carotid stenosis and infarct volume in ischemic stroke patients, Med Sci Monit 22 (2016) 4954–4959, https://doi.org/10.12659/msm.898112.

[2] A. Saxena, E.Y.K. Ng, S.T. Lim, Imaging modalities to diagnose carotid artery stenosis: progress and prospect, Biomed. Eng. Online 18 (1) (2019) 66, https://doi.org/10.1186/s12938-019-0685-7.

[3] J.J. Warner, R.A. Harrington, R.L. Sacco, M.S.V. Elkind, Guidelines for the early management of patients with acute ischemic stroke: 2019 update to the 2018 guidelines for the early management of acute ischemic stroke, Stroke 50 (12) (2019) 3331–3332, https://doi.org/10.1161/STROKEAHA.119.027708.

[4] A. Goddi, C. Bortolotto, M.V. Raciti, I. Fiorina, L. Aiani, G. Magistretti, A. Sacchi, C. Tinelli, F. Calliada, High-frame rate vector flow imaging of the carotid bifurcation in healthy adults: comparison with color Doppler imaging, J. Ultrasound Med. 37 (9) (2018) 2263–2275, https://doi.org/10.1002/jum.14579.

[5] A.M. Malek, S.L. Alper, S. Izumo, Hemodynamic shear stress and its role in atherosclerosis, JAMA 282 (1999) 2035–2042, https://doi.org/10.1001/jama.282.21.2035.

[6] C.J. Slager, J.J. Wentzel, F.J. Gijsen, J.C. Schuurbiers, A.C. van der Wal, A.F. vander Steen, et al., The role of shear stress in the generation of rupture prone vulnerable plaques, Nat. Clin. Pract. Cardiovasc. Med. 2 (2005) 401–407, https://doi.org/10.1038/ncpcardio0274.

[7] P. Eshtehardi, A.J. Brown, A. Bhargava, C. Costopoulos, O.Y. Hung, M.T. Corban, et al., High wall shear stress and high-risk plaque: an emerging concept, Int J Cardiovasc Imaging 33 (2017) 1089–1099, https://doi.org/10.1007/s10554-016-1055-1.

[8] A. Tuenter, M. Selwaness, A. Arias Lorza, J.C.H. Schuurbiers, L. Speelman, M. Cibis, A. van der Lugt, M. de Bruijne, A.F.W. van der Steen, O.H. Franco, M. W. Vernooij, J.J. Wentzel, High shear stress relates to intraplaque haemorrhage in asymptomatic carotid plaques, Atherosclerosis 251 (2016) 348–354, https://doi.org/10.1016/j.atherosclerosis.2016.05.018.

[9] A.M. Moerman, S. Korteland, K. Dilba, K. van Gaalen, D.H.J. Poot, A. van Der Lugt, H.J.M. Verhagen, J.J. Wentzel, A.F.W. van Der Steen, F.J.H. Gijsen, K. Van der Heiden, The correlation between wall shear stress and plaque composition in advanced human carotid atherosclerosis, Front. Bioeng. Biotechnol. 9 (2022) 828577, https://doi.org/10.3389/fbioe.2021.828577.
[10] E. Yamamoto, V. Thondapu, E. Poon, T. Sugiyama, F. Fracassi, J. Dijkstra, H. Lee, A. Ooi, P. Barlis, I.K. Jang, Endothelial shear stress and plaque erosion: a computational fluid dynamics and optical coherence tomography study, JACC Cardiovasc Imaging 12 (2) (2019) 374–375, https://doi.org/10.1016/j.jcmg.2018.07.024.
[11] T. Saho, H. Onishi, Quantitative analysis of wall shear stress for human carotid bifurcation at cardiac phases by the use of phase contrast cine magnetic resonance imaging: computational fluid dynamics study, Nihon Hoshasen Gijutsu Gakkai Zasshi 1 (12) (2015) 1157, https://doi.org/10.6009/jjrt.2015_JSRT_71.12.1157.
[12] F.O. Mutluer, N. van der Velde, J. Voorneveld, J.G. Bosch, J.W. Roos-Hesselink, R.J. van der Geest, A. Hirsch, A. van den Bosch, Evaluation of intraventricular flow by multimodality imaging: a review and meta-analysis, Cardiovasc. Ultrasound 19 (1) (2021) 38, https://doi.org/10.1186/s12947-021-00269-8.
[13] H. Hayashi, K. Akiyama, K. Itatani, S. DeRoo, J. Sanchez, G. Ferrari, P.C. Colombo, K. Takeda, I.Y. Wu, A. Kainuma, H. Takayama, A novel in vivo assessment of fluid dynamics on aortic valve leaflet using epi-aortic echocardiogram, Echocardiography 37 (2) (2020) 323–330, https://doi.org/10.1111/echo.14596.
[14] Y. Cai, X. Wei, C. Li, X. Zhang, H. Tang, L. Rao, New echocardiographic method for chronic aortic regurgitation: diastolic retrograde ratio in the descending aorta by vector flow mapping, Int J Cardiovasc Imaging 35 (3) (2019) 461–468, https://doi.org/10.1007/s10554-018-1471-5.
[15] Y. Nakajima, T. Hozumi, K. Takemoto, S. Fujita, T. Wada, M. Kashiwagi, K. Shimamura, Y. Shiono, A. Kuroi, T. Tanimoto, T. Kubo, A. Tanaka, T. Akasaka, Noninvasive estimation of impaired left ventricular untwisting velocity by peak early diastolic intra-ventricular pressure gradients using vector flow mapping, J. Echocardiogr. 19 (3) (2021) 166–172, https://doi.org/10.1007/s12574-021-00520-1.
[16] C. Karmonik, J. Bismuth, M.G. Davies, D.J. Shah, H.K. Younes, A.B. Lumsden, A computational fluid dynamics study pre- and post-stent graft placement in an acute type B aortic dissection, Vasc Endovascular Surg 45 (2) (2011 Feb) 157–164, https://doi.org/10.1177/1538574410389342. Epub 2010 Dec 13. PMID: 21156714.
[17] J. Febina, M.Y. Sikkandar, N.M. Sudharsan, Wall shear stress estimation of thoracic aortic aneurysm using computational fluid dynamics, Comput. Math. Methods Med. 2018 (2018 Jun 3) 7126532, https://doi.org/10.1155/2018/7126532. PMID: 30008797; PMCID: PMC6008891.
[18] A. Goddi, C. Bortolotto, I. Fiorina, M.V. Raciti, M. Fanizza, E. Turpini, G. Boffelli, F. Calliada, High-frame rate vector flow imaging of the carotid bifurcation, Insights Imaging 8 (3) (2017) 319–328, https://doi.org/10.1007/s13244-017-0554-5.
[19] Y. Qiu, Y. Dong, F. Mao, Q. Zhang, D. Yang, K. Chen, S. Shi, D. Zuo, X. Tian, L. Yu, W.P. Wang, High-frame rate vector flow imaging technique: initial application in evaluating the hemodynamic changes of carotid stenosis caused by atherosclerosis, Front Cardiovasc Med 8 (2021) 617391, https://doi.org/10.3389/fcvm.2021.617391.
[20] C. North American Symptomatic Carotid Endarterectomy Trial, H.J.M. Barnett, D.W. Taylor, R.B. Haynes, D.L. Sackett, S.J. Peerless, et al., Benefificial effffect of carotid endarterectomy in symptomatic patients with high-grade carotid stenosis, N. Engl. J. Med. 325 (1991) 445–453, https://doi.org/10.1056/NEJM199108153250701.
[21] Y. Du, A. Goddi, C. Bortolotto, Y. Shen, A. Dell'Era, F. Calliada, L. Zhu, Wall shear stress measurements based on ultrasound vector flow imaging: theoretical studies and clinical examples, J. Ultrasound Med. 39 (8) (2020) 1649–1664, https://doi.org/10.1002/jum.15253.
[22] X. Zhang, Z. Jiao, Z. Hua, H. Cao, S. Liu, L. Zhang, C. Lian, C. Li, Z. Li, Localized elevation of wall shear stress is linked to recent symptoms in patients with carotid stenosis, Cerebrovasc. Dis. 52 (3) (2023) 283–292, https://doi.org/10.1159/000526872. Epub 2022 Oct 21. PMID: 36273462.
[23] T. Kamimura, S. Aoki, T. Nezu, F. Eto, Y. Shiga, M. Nakamori, E. Imamura, T. Mizoue, S. Wakabayashi, H. Maruyama, Association between carotid wall shear stress-based vascular vector flow mapping and cerebral small vessel disease, J Atheroscler Thromb 30 (9) (2023 Sep 1) 1165–1175, https://doi.org/10.5551/jat.63756. Epub 2022 Nov 4. PMID: 36328567; PMCID: PMC10499442.
[24] L. He, Y. Cai, Y. Feng, W. Wang, T. Feng, E. Shen, S. Yang, Utility of vector flow mapping technology in quantitative assessment of carotid wall shear stress in hypertensive patients: a preliminary study, Front Cardiovasc Med 9 (2022 Oct 28) 967763, https://doi.org/10.3389/fcvm.2022.967763. PMID: 36386366; PMCID: PMC9649775.
[25] N. Hariri, T. Russell, G. Kasper, et al., Shear rate is a better marker of symptomatic ischemic cerebrovascular events than velocity or diameter in severe carotid artery stenosis, J. Vasc. Surg. 69 (2) (2019) 448–452, https://doi.org/10.1016/j.jvs.2018.04.036.
[26] G. Goudot, J. Poree, O. Pedreira, et al., Wall shear stress measurement by ultrafast vector flow imaging for atherosclerotic carotid stenosis, Ultraschall der Med. 42 (3) (2021) 297–305, https://doi.org/10.1055/a-1060-0529.
[27] C.R. Lee, J.A. Luzum, K. Sangkuhl, R.S. Gammal, M.S. Sabatine, C.M. Stein, D.F. Kisor, N.A. Limdi, Y.M. Lee, S.A. Scott, J.S. Hulot, D.M. Roden, A. Gaedigk, K. E. Caudle, T.E. Klein, J.A. Johnson, A.R. Shuldiner, Clinical pharmacogenetics implementation consortium guideline for CYP2C19 genotype and clopidogrel therapy: 2022 update, Clin. Pharmacol. Ther. 112 (5) (2022 Nov) 959–967, https://doi.org/10.1002/cpt.2526. Epub 2022 Feb 8. PMID: 35034351; PMCID: PMC9287492.
[28] R.A. Wilke, L.B. Ramsey, S.G. Johnson, W.D. Maxwell, H.L. McLeod, D. Voora, R.M. Krauss, D.M. Roden, Q. Feng, R.M. Cooper-Dehoff, L. Gong, T.E. Klein, M. Wadelius, M. Niemi, Clinical Pharmacogenomics Implementation Consortium (CPIC), The clinical pharmacogenomics implementation consortium: CPIC guideline for SLCO1B1 and simvastatin-induced myopathy, Clin. Pharmacol. Ther. 92 (1) (2012 Jul) 112–117, https://doi.org/10.1038/clpt.2012.57. Epub 2012 May 23. PMID: 22617227; PMCID: PMC3384438.
[29] M. Leusink, A.H. Maitland-van der Zee, B. Ding, F. Drenos, E.P. van Iperen, H.R. Warren, M.J. Caulfield, L.A. Cupples, M. Cushman, A.D. Hingorani, R. C. Hoogeveen, G.K. Hovingh, M. Kumari, L.A. Lange, P.B. Munroe, F. Nyberg, P.J. Schreiner, S. Sivapalaratnam, P.I. de Bakker, A. de Boer, B.J. Keating, F. W. Asselbergs, N.C. Onland-Moret, A genetic risk score is associated with statin-induced low-density lipoprotein cholesterol lowering, Pharmacogenomics 17 (6) (2016 Apr) 583–591, https://doi.org/10.2217/pgs.16.8. Epub 2016 Apr 5. PMID: 27045730; PMCID: PMC5558527.
[30] J. Malik, L. Novakova, A. Valerianova, et al., Wall shear stress alteration: a local risk factor of atherosclerosis, Curr Atheroscler Rep 24 (3) (2022) 143–151, https://doi.org/10.1007/s11883-022-00993-0.
[31] M. Mahmoudi, A. Farghadan, D.R. McConnell, et al., The story of wall shear stress in coronary artery atherosclerosis: biochemical transport and mechanotransduction, J. Biomech. Eng. 143 (4) (2021) 041002, https://doi.org/10.1115/1.4049026.